Journal of Cranio-Maxillo-Facial Surgery xxx (xxxx) xxx

Contents lists available at ScienceDirect

Journal of Cranio-Maxillo-Facial Surgery

journal homepage: www.jcmfs.com

Lateral pterygoid muscle enthesis reconstruction in total temporomandibular joint replacement: An animal experiment with radiological correlation

Nikolas De Meurechy [a, b, *], Denis Verwilghen [c], Yannick De Brucker [d], Bert Van Thielen [d], Maurice Y. Mommaerts [a, e]

[a] European Face Centre (head Prof. M.Y.Mommaerts), Universitair Ziekenhuis Brussel, Brussels, Belgium
[b] Doctoral School of Life Sciences and Medicine (head Prof. L Van Grunsven), Vrije Universiteit Brussel, Brussels, Belgium
[c] Camden Equine Centre, University Veterinary Teaching Hospital (head Prof. Dr. D. Verwilghen), School of Veterinary Sciences, Faculty of Science, University of Sydney, Sydney, Australia
[d] Department of Radiology (head Prof. J.Demeye), Universitair Ziekenhuis Brussel, Brussels, Belgium
[e] CADskills BV, Ghent, Belgium

ARTICLE INFO

Article history:
Paper received 3 April 2020
Received in revised form
15 November 2020
Accepted 31 January 2021
Available online xxx

Keywords:
Pterygoid muscles
Temporomandibular joint
Joint prosthesis
Animal experiment
Arthroplasty
Computed tomography

ABSTRACT

A novel total temporomandibular joint replacement (TMJR) was developed with CADskills BV (Ghent, Belgium), aiming to achieve reinsertion of the (LPM) onto a scaffold in the implant. In order to investigate the possibility of reinsertion of the LPM, an animal experiment was conducted.

An in vivo sheep experiment was conducted, which involved implanting sheep with a TMJR. Clinical parameters were recorded regularly and computed tomography (CT) scan images of two randomly selected sheep per scan were made at 1, 3, and 6 months. After 9.5 months, the sheep were euthanized, and CT scans of all animals were performed in order to evaluate the LPM's enthesis.

A total of 13 sheep were implanted with a TMJR. One sheep was used as a sham. Radiographs revealed four outcome types of enthesis reconstruction. In four sheep, there was no reconstruction between the implant and the LPM. In three sheep, there was a purely soft tissue connection of 0.5–0.9 mm (average 0.7 mm) between the ostectomized bony LPM insertion and the implant's lattice structure. A combination of partial bony and partial soft tissue enthesis attachment (0.3–0.5 mm, average 0.4 mm) was found in three sheep. A bony ingrowth of the enthesis into the scaffold occurred in two sheep. A secondary bony connection between the mandible and the insertion of the LPM was found in 10 of 13 sheep. Four fossa components were found to be displaced, yet TMJ function remained in these ewes. The heterotopic ossification that was seen may be a confounding factor in these results.

This in vivo experiment showed promising results for improving the current approach to TMJR with the possibility of restoring the laterotrusive function. The fossa displacement was considered to be due to insufficient fixation and predominant laterotrusive force not allowing for proper osseointegration. Further optimization of the reattachment technique, scaffold position and surface area should be done, as well as trials in humans to evaluate the effect of proper revalidation.

© 2021 European Association for Cranio-Maxillo-Facial Surgery. Published by Elsevier Ltd. All rights reserved.

1. Introduction

Since the first total temporomandibular joint replacement (TMJR) method was conceived in 1965 by Christensen, many more systems have been devised. A total of 27 different TMJR systems are curren:tly in use (De Meurechy and Mommaerts, 2018; Elledge et al., 2019). However, none provides for reinsertion of the lateral

* Corresponding author. European Face Centre, Universitair Ziekenhuis Brussel, Laarbeeklaan 101, 1090, Brussel, Belgium.
E-mail address: de.meurechy.n@gmail.com (N. De Meurechy).

https://doi.org/10.1016/j.jcms.2021.01.029
1010-5182/© 2021 European Association for Cranio-Maxillo-Facial Surgery. Published by Elsevier Ltd. All rights reserved.

Please cite this article as: N. De Meurechy, D. Verwilghen, Y. De Brucker *et al.*, Lateral pterygoid muscle enthesis reconstruction in total temporomandibular joint replacement: An animal experiment with radiological correlation, Journal of Cranio-Maxillo-Facial Surgery, https://doi.org/10.1016/j.jcms.2021.01.029

pterygoid muscle (LPM), which is surgically detached during the condylar resection phase.

The importance of the LPM is apparent when examining the different phases of mastication. The incisor and canine teeth first cut and tear the food, respectively. The premolars and molars then crush and chew the food, which is ground to the point at which it can easily be swallowed and further improve digestion. Mastication efficiency refers to the number of chews necessary to grind down the food. It is dependent on good articular and muscular function and on the individual's dental condition (Bates et al., 1976; Kijak et al., 2017).

The lateral pterygoid muscle participates in the cutting and tearing phases of mastication by performing protrusion. It also performs laterotrusive motions during the chewing and grinding phase. Laterotrusive motions occur via unilateral contraction of the LPM. Protrusion results from bilateral contraction of the lateral pterygoid muscle. Loss of the lateral pterygoid muscle results in impaired laterotrusive and protrusive functions. For example, the average laterotrusion in humans is 10 mm, but a long-term follow-up study by Mercuri et al. (2002) found that significant post-operative decreases in laterotrusion occur after TMJR procedures. They reported an average laterotrusion of 3.07 mm (95%, 2.09–4.04) to the contralateral side after unilateral, right TMJR and 3.04 mm (95% CI, 1.98–4.10) after unilateral, left TMJR procedures. Similar findings were reported by Dimitroulis (2014). They found that laterotrusion can be limited to a mean value of 1.6 mm (range 0–2.9 mm). Correct mastication occurs bilaterally. During unilateral mastication, the TMJs are subjected to an uneven load, and further deterioration of the TMJ that experiences most of the load can result (Mommaerts 2019).

In an attempt to reinstall laterotrusive movement after joint replacement, Mommaerts (2019) reconstructed the LPM enthesis using direct reinsertion of the muscle onto the TMJR in three patients. He proposed the use of a condylar lattice structure in the pterygoid fovea of the mandibular component of the TMJR to which the enthesis can be reattached. This structure is first filled with crushed autologous bone and concentrated bone marrow aspirate, to promote the formation of bone and collagenous tissue after reattachment of the LPM. Three patients were treated using this “reattachment” technique. The study findings indicated that under the correct conditions, use of a condylar lattice structure resulted in a good outcome.

With these findings serving as clinical proof of concept, we optimized this patient-specific TMJR and designed an animal model to further investigate the possibility of reconstruction of the lateral pterygoid muscle enthesis without the addition of bone marrow aspirate as well as to evaluate overall TMJR performance.

2. Materials and methods

2.1. In vivo test subjects

There are biomechanical and morphological differences between the TMJs of different species. Therefore, compared with other species, some are more suitable for use as experimental animal models (Angelo et al., 2016). Primates such as monkeys are very similar to humans in both morphological and biomechanical TMJ characteristics, but their use is severely limited by ethics. While both sheep and goat TMJs show morphological similarities to the human TMJ, the total amount of daily mastication of goats is relatively limited compared with sheep. The latter spend an average of 4 h per day eating at 128 mastication cycles per minute and 8–9 h ruminating at 100 cycles per minute (Domingue et al., 1991). This high number of mastication cycles per day allows for reductions in the total period of in vivo evaluation, especially in terms of wear and overall performance (i.e., except for materials ageing), making them more suitable for this experiment. The total duration for the experiment was set at 288 days, which is equivalent to 22 years of human function (Verplancke et al., 2011).

Fourteen sheep (Swifter crossbreed) were acquired after gaining ethical committee approval (License nr. LA 1210576) for the study (code of approval EC MxCl 2018-090). All ewes were between 2 and 5 years of age, weighed between 52 and 86 kg (average weight, 73.4 kg), and had no teeth missing (Table 1). The ewes were allowed to move freely in a meadow up until the day of surgery. After the surgery, they were kept in solitary confinement for 1 week. After this first week, they were put together in a larger indoor confinement area.

In the first series of surgeries, two sheep were operated upon in April 2018. An animal-specific unilateral TMJR was placed in one sheep. The other sheep was used for the sham surgery. The sham surgery consisted of the same surgical approach with dissection of the joint, but no implant was placed, nor was a condylectomy performed. We did not include the sham in this article, as the LPM was left intact. The 12 other sheep were operated upon 2 months later, after the surgical technique was optimized based on the experience with the first two sheep.

2.2. Implant

To design the implants, a computed tomography (CT) scan was made of each sheep 6 weeks before the surgery date. The CT data were provided in Digital Imaging and Communications in Medicine (DICOM) format to CADskills BV engineers (Ghent, Belgium). They reconstructed the images to a standard template library (STL) file, performed the resections virtually, and then designed the implants using Geomagic Freeform Plus (3D Systems, Rock Hill, SC, USA). All implants were designed for the left TMJ, and the implant design, number of screws, and screw diameters were as similar to the human design as possible. The lengths and positions of the screws were predetermined during implant design and were based on the amounts of bone and the adjacent anatomical structures (e.g. the inferior alveolar nerve). Subsequently, both the skull and the implant associated with the first sheep were three-dimensionally printed using a fused deposit model three-dimensional (3D) printer (Makerbot, MakerBot Industries, Brooklyn, NY, USA) and a stereolithographic resin 3D-printer (Formlabs II, Formlabs, Sommerville, MA, USA), respectively (Fig. 1). The resulting prints were used to make further implant design improvements.

The skull base component consisted of two parts. One part was printed from a medical grade titanium alloy grade 23 extra low interstitials (ELI-23), which fit over the glenoid fossa and articular eminence and was screw-fixed to the zygomatic arch. The other part faced the condyle and was made out of a concave computer numeric controlled milled vitamin E–enriched ultra–high-molecular weight polyethylene (UHMWPE), which was then ɣ-radiated to increase the amount of crosslinks within the polyethylene. Both parts were connected via non-disclosed pressure, time, and temperature settings in a scaffold layer at the condyle-facing side of the titanium component. The titanium was alumina (550-μ grit) micro-shot-peened and oxalic acid etched to promote osseointegration. Fixation was performed using five titanium screws (Gr 5, diameter 2.0 mm, length 5–13 mm; Surgi-Tec NV, Ghent, Belgium) (Fig. 2). In addition to a lattice structure at the bony interface, the ELI-23 titanium alloy ramal component had a large connecting lattice structure in the condylar neck and a tunnel through the condylar neck with a small hook-like extension on the lateral side. The tunnel and hook were used to thread PDS 0 suture material, which was passed through the preserved bony or fibrocartilaginous enthesis of the LPM and fixed to the hook-like extension. The lattice

Table 1
Sheep number and weight (kg) at pre-op, 1 week post-op, 1, 3, 6, 9, and 9.5 months post-operatively (post-op).

Sheep no.	Pre-op	1 wk post-op	3 mo post-op	6 mo post-op	9 mo post-op	9.5 mo post-op
3520	86.6	78.8	73.5	76.6	71.4	74.2
8087	61.4	53.8	52.1	53.9	59.8	59.6
2177	79.4	71.2	67.5	72.3	78.2	79.9
5158	72.3	63.3	66.8	70.9	77.6	80.1
2549	63.3	55.8	55.9	61.3	63.2	63.9
4249	75.8	65.5	61.5	62.5	64	63.6
0032	64.2	55.9	51.9	58.7	59.1	60.4
7998	83.9	76.2	68.7	70.8	75.8	77.2
4246	74.6	66.3	66.2	71.8	77.3	76.1
1724	83.9	76.3	75.8	84.3	90	91.9
4248	69.2	62.4	65.1	68.6	72.4	72.9
8787	52.3	50	45.6	47.3	48.6	47.7
4473	86	77.2	75.2	78.4	81.7	83.2
0075	74.3	68.3	78	80.2	86.9	87.6

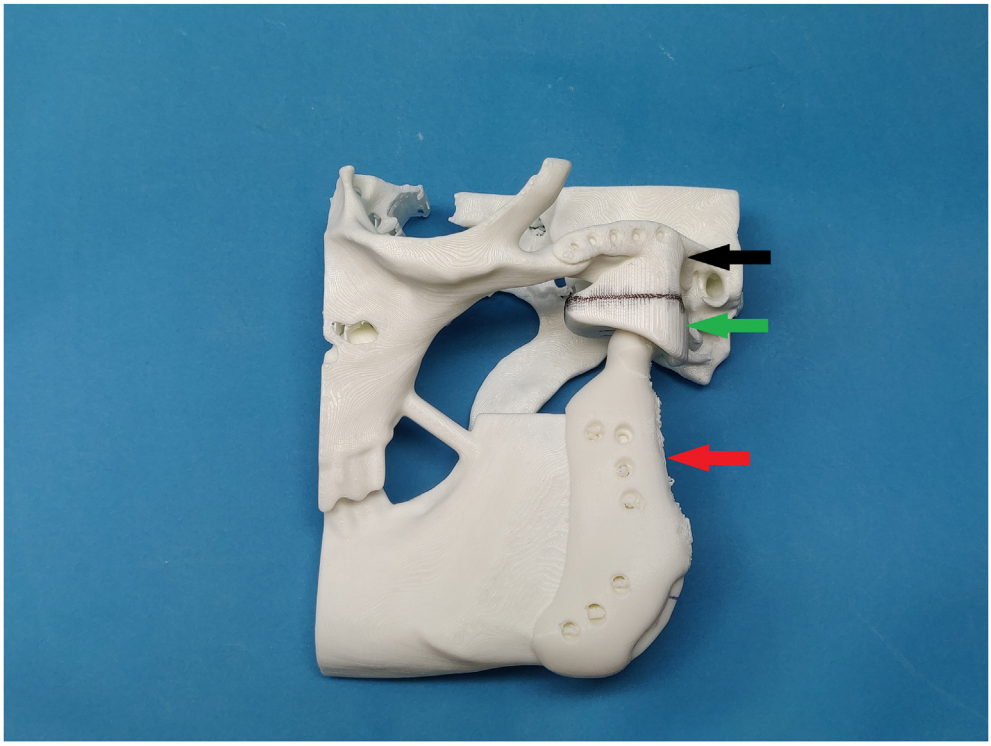

Fig. 1. Fused deposit three-dimensional model of a partial sheep's skull with the total temporomandibular joint replacement (TMJR). Red arrow: Mandibular component of the TMJR; green arrow: ultra–high-molecular weight polyethylene component of the TMJR fossa component; black arrow: titanium component of the TMJR fossa component.

structure interior (500-μ interconnected pores with a diamond unit cell structure) provided an optimal region for bony union of the enthesis with the transplanted bone particles (Fig. 3). Six of the ramal components' condylar heads were treated using a HadSat® diamond-like carbon coating; seven remained untreated. Fixation of the ramal component was performed using an average of six titanium Gr 5 screws (Surgi-Tec, Ghent, Belgium; diameter 2.3 mm, length 13–17 mm).

2.3. Surgical protocol

Each ewe was first sedated using xylazine (0.1 mg/kg) and then shaved over the left mandible. Anesthesia was subsequently given using ketamine (4 mg/kg) and midazolam (0.2 mg/kg) for induction. The sheep was then intubated with a cuffed tube, and anesthesia was maintained using mechanical ventilation with an oxygen–isoflurane mixture. Surgical site was aseptically prepared. Xylocaine (1%) with 1/80.000 epinephrine was locally infiltrated at the jaw angle and over the zygomatic arch to achieve local vasoconstriction and anesthesia.

A 4-cm incision was made over the posterior lower border of the mandible. The lateral surface and the angle of the mandible were exposed. A pre-auricular, s-shaped incision inferior to the zygomatic arch was used to expose the TMJ, and a subperiosteal connection was made with the previously prepared lateral side of the vertical ramus. An ELI-23 titanium cutting guide was screw-fixed to the vertical ramus to aid in performing the condylectomy. The joint space was then opened and the temporomandibular disc was removed. The condylectomy was then performed. The bony attachment of the lateral pterygoid muscle to the condyle was preserved in six sheep. In seven sheep, only the fibrocartilaginous part of the muscle insertion was unintentionally preserved. In two

Fig. 2. Fossa component.

sheep, it was unclear whether either or both could be preserved. Compared with humans, it was difficult to keep the tendon inserted in the pterygoid fovea during dissection and removal of the rest of the condylar process. In our experience, in humans there is a larger bony insertion for the LPM to attach to the condyle. Sheep have a mostly fibrotic insertion into both the intra-articular disc and condyle. A PDS 0 suture (Ethicon, Sommverville, NJ, USA) was threaded through either the bony part of the enthesis or the fibrocartilaginous insertion.

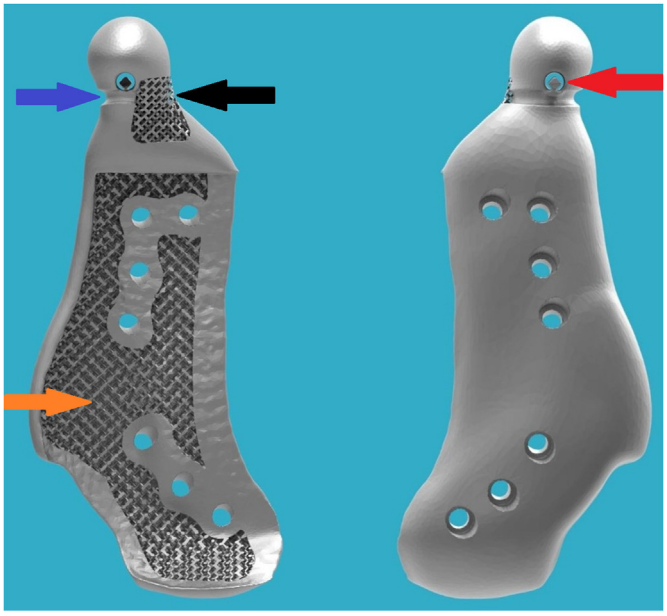

Fig. 3. Three-dimensional rendering of the ramal component with lattice structure and tunnel for fixation of the enthesis. Red arrow: subcondylar tunnel and hook-like extension for fixation of the enthesis; blue arrow: subcondylar groove to guide enthesis' sutures; black arrow: lattice structure for enthesis' bony ingrowth; orange arrow: lattice structure for mandibular bony ingrowth into the ramal component.

The fossa component was first placed using a dummy version and was fixed using five screws. Bone from the resected condyle was harvested, crushed, and mixed with fibrin sealant (Tisseel, Baxter, Deerfield, IL, USA). It was then manually pressed into the pterygoid fovea scaffold (Fig. 4a, b). The ramal component was then fit in place while the PDS 0 was threaded through the subcondylar tunnel and then tied to the small hook as soon as the ramal component was fixed to the mandible (Fig. 5). Using the suture to pull the bony enthesis to the bone in the scaffold proved difficult because the UHMWPE of the fossa component was interfering in a caudal direction. All UHMWPE parts were scalpel-reduced at the anteromedial side to facilitate routing the enthesis or tendon/fibrocartilaginous part of the disc. This excess volume of UHMWPE resulted from using the human type of fossa UHMWPE design, in which there is to reckon with a lower total muscle mass of the lateral pterygoid muscle, resulting in less spherical obstruction. As we were not able to completely segment the LPM during the design process of the implant, this led to a slight underestimation of the total muscle volume. All UHMWPE parts were altered in such a fashion that it did not affect the articulating surface, and the LPM did not experience any obstruction after correction.

The articular capsule and soft tissues were closed in multiple layers and a compressive bandage was placed for 1 week. Peroperative pain control was achieved using buprenorphine (6 μg/kg) administered via the intravenous route.

2.4. Post-operative protocol and euthanasia

Each ewe was kept alone during the first post-operative week. Heart rate, respiratory rate, body temperature, dietary status (appetite, whether water consumed), and excretions were recorded daily. The compressive bandage was replaced daily, and the wound was examined for swelling and signs of infection. Blood samples were taken on a daily basis during the first postoperative week to check the white cell count and formula. Ionogram and inflammatory parameters were checked twice the first week. If necessary, meloxicam (0.5 mg/kg) was used for pain management. Buprenorphine (5 μg/kg) was added if meloxicam was insufficient for proper pain control. During the first week, only soft, moistened food was given to the ewes. After 1 week, they were confined together in a large indoor pen, and blood samples were taken and a clinical examination was performed once per week.

In one sheep, submentovertical and lateral post-operative radiographic images were acquired shortly after implantation to investigate some observed mandibular asymmetry. Both images showed correct placement of the implant. At 1 month, 3 months, and 6 months after surgery, CT images were taken of two randomly selected sheep to evaluate implant position and condition, bony ingrowth into the scaffolds, and attachment of the enthesis.

The 14 animals were euthanized 9.5 months after implantation. A clinical evaluation was done and blood samples were taken before euthanasia. Xylazine (0.1 mg/kg) was administered for induction and heparin (300 IU/kg) was given to prevent coagulation. Induction was done using a combination of ketamine (4 mg/kg) and midazolam (0.2 mg/kg). The product administered to achieve euthanasia cannot be disclosed per agreement with the animal laboratory. After euthanasia, each ewe was decapitated, the skull was cut in half, and the right side was disposed of, except for three randomly selected sheep. In these sheep, specimens were kept for comparative analysis. Further decomposition of the left side of the skull was performed by skinning the specimen, removing the neurocranium, and removing the anterior half of the mandible and maxilla. The eye and upper half of the orbit were also removed.

Specimens were fixed using immersion in formaldehyde (4%) for 2 months. A post-mortem CT scan of each specimen was then

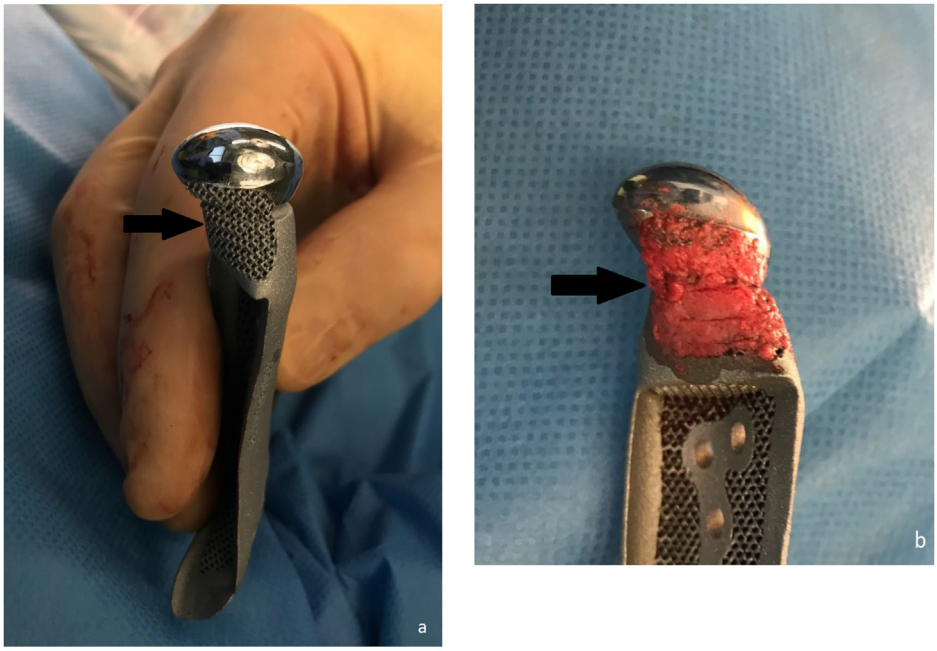

Fig. 4. (a) Lattice structure before bone application (black arrow). (b) Lattice structure with mixture of bone and fibrin sealant (black arrow).

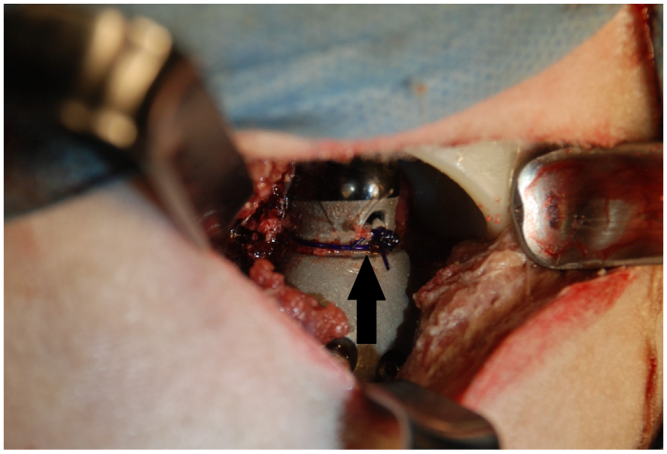

Fig. 5. Mandibular component fixed with enthesis fixed through the subcondylar tunnel. Black arrow: PDS 0 suture (Ethicon, Sommverville, NJ, USA) threaded through the subcondylar tunnel, run around the subcondylar groove, and fixed to the hook-like extension.

performed (slice thickness 0.7 mm, 500 mAs, 120 kV, reconstruction thickness <1 mm; Revolution, General Electric, Fairfield, CT, USA). The images were analyzed using Agfa IMPAX 6, Agfa-Gevaert NV, Mortsel, Belgium) and were reconstructed into STL-files and 3D-renders using Mimics inPrint 3.0 (Materialise, Haasrode, Belgium). The goal of the imaging analysis was to determine the presence or absence of enthesis reconstruction.

The peri-articular tissues were resected, stained using hematoxylin–eosin, and embedded in paraffin. The goal was to examine local adverse tissue reaction to the implant materials, infection, and wear-induced synovitis, which will be reported separately. The CT scan and 3D reconstruction were used to determine where and how sections should be made through the lateral pterygoid muscle and its enthesis, and through the implant, to allow for histological analysis of the enthesis and its connection to the scaffold. Masson-Goldner (M-G) trichrome stain was used for the histology (Rentsch et al., 2014).

3. Results

3.1. Weight and cinematics

During the post-operative period, each sheep was weighed and evaluated weekly. The average preoperative weight was 73.4 kg, and an average loss of 8.4 kg occurred during the first post-operative week. The average weight then declined even more by 3 months after implantation, but then increased and was 72.7 kg at the end of the observation period (Table 1).

Sheep have a preferred side for rumination, but they will switch sides (Ángelo et al., 2018). To ascertain that the ewes did not perform only left-sided laterotrusion, video recordings of the right-sided rumination movements of two randomly selected sheep were made before surgery. Videos of 2 sheep that were pre-operatively randomly selected, were also made at 1 week, 3 months, and 9 months after surgery. They revealed the presence of laterotrusive movement to the right side, which indicated unilateral contraction of the LPM on the operated side. The LPM was still attached to the implant and allowed for laterotrusive movement to the contralateral side (Video 1-3).

Supplementary video related to this article can be found at https://doi.org/10.1016/j.jcms.2021.01.029

3.2. Radiology

The CT scans were evaluated for the presence of a bony insertion of the LPM that was in contact with the subcondylar lattice structure. The operative notes described whether a bony piece of the enthesis or whether fibrocartilaginous tissue was re-attached to the implant (Table 2).

The follow-up scans at 1 month after surgery revealed good positioning of the fossa component in ewe 1724. The ramal component was not yet well-integrated with the mandible. However, as expected, there was callus formation between the mandible

Table 2
Per-operative reconstruction and post-operative CT evaluation connection between the lateral pterygoid muscle (LPM) and the implant scaffold.

Sheep no.	Per-operative	1 mo post-op	3 mo post-op	6 mo post-op	Post-mortem
3520	Bony				Soft tissue
8087	Unclear	Bone			Bone
2177	Bony			Absent	Absent
5158	Unclear		Bone		Bone + Soft tissue
2549	Fibrocartilaginous			Absent	Absent
4249	Fibrocartilaginous				Bone
0032	Fibrocartilaginous				Soft tissue
7998	Bony		Absent		Absent
4246	Bony				Bone + Soft tissue
1724	Bony	Soft tissue			Soft tissue
4248	Bony				Bone + Soft tissue
8787	Fibrocartilaginous				Absent
4473	Fibrocartilaginous				[a]Absent
0075	SHAM	SHAM	SHAM	SHAM	SHAM

Post-op = postoperatively.
[a] Due to dissection.

and the ramal component. There was also a soft tissue connection with a thickness of 3 mm between the implant and the enthesis. In comparison, the post-mortem scan showed both bony and soft tissue connections between the implant and the scaffold. This result can be explained by formation of heterotopic bone surrounding the ramal component, which provided additional support and stability and allowed for better integration. The results for the second sheep that was scanned, ewe 8087, also indicated there was good positioning of both components and initial osseointegration of the ramal component. There was a good attachment of the enthesis onto the scaffold, and there were several centers of early, non-mineralized bone between the enthesis and scaffold and the enthesis and the mandible. Early heterotopic osseous centers lateral to the mandibular implant were also found (Table 3).

The 3-month in vivo CT scans of the sheep marked 7998 revealed that despite the intra-operative bony connection that was achieved, the enthesis was no longer connected to the implant. Instead, there was an osseous connection between the mandible and the enthesis of the LPM. Both the fossa and ramal component were well positioned, and there was good integration of the ramal component. The second sheep that was scanned at 3 months after surgery, ewe 5158, had good positioning of both the fossa and ramal component, good integration of the ramal component, and a bony connection between the attached enthesis and the implant. As with the other sheep, there was also a bony connection between the mandible and the enthesis. Although both TMJR components were well-positioned and integrated, heterotopic bone was formed laterally from the implant and appeared to connect the mandible to the skull base. A fracture of this heterotopic bone prevented joint ankylosis. This fracture was likely due to continued movement of the mandible.

One of the two sheep scanned at 6 months after surgery, marked 2177, had a bony connection between the enthesis and the mandible, as was found in the previous two sheep. However, there was no bony connection between the enthesis and the scaffold. There was heterotopic bone formation around the lateral side of both the ramal and the fossa components. There was also a slight latero-inferior displacement of the fossa component, showing non-integration onto the articular tubercle. The scan of the second sheep, ewe 2549, revealed good positioning of both TMJR

Table 3
Type of connection formed post-mortem between the mandible and lateral pterygoid muscle (LPM), based on computed tomographic evaluation.

Sheep no.	Connection type
3520	Soft tissue connection between the implant scaffold and reattached enthesis Bony connection between the mandible and reattached enthesis
8087	Bony connection between the implant scaffold and reattached enthesis Bony connection between the mandible and reattached enthesis
2177	Bony connection between the mandible and reattached enthesis
5158	Partial bony and soft tissue connection between the implant scaffold and reattached enthesis Bony connection between the mandible and reattached enthesis
2549	Absent
4249	Bony connection between the implant scaffold and reattached enthesis Bony connection between the mandible and reattached enthesis
0032	Soft tissue connection between the implant scaffold and reattached enthesis Bony connection between the mandible and reattached enthesis
7998	Bony connection between the mandible and reattached enthesis
4246	Partial bony and soft tissue connection between the implant scaffold and reattached enthesis Bony connection between the mandible and reattached enthesis
1724	Soft tissue connection between the implant scaffold and reattached enthesis Bony connection between the mandible and reattached enthesis
4248	Partial bony and soft tissue connection between the implant scaffold and reattached enthesis Bony connection between the mandible and reattached enthesis
8787	Absent
4473	[a]Absent
0075	Sham

[a] Due to dissection.

components, but there was no enthesis reconstruction with osseous or fibrotic characteristics.

The post-mortem CT scans revealed four different conditions (Table 3). In four of the ewes, there was no reconstruction between the implant and the LPM, with complete absence or a large distance between the LPM and the implant. In one case, the post-operative specimen was poorly dissected and there was destruction of the enthesis reconstruction as a result of this. In two of the sheep, the ostectomized bony enthesis was sutured to the scaffold in the condylar neck during the implantation surgery. In the other two cases, the fibrocartilaginous tissue was re-attached.

Three sheep had purely soft tissue connections between the ostectomized bony insertion of the LPM and the lattice structure of the implant. Two of these three sheep had a per-operative bony reattachment, and in one sheep the fibrocartilaginous tissue was re-attached to the subcondylar scaffold (Fig. 6).

Three sheep had a combination of partial bony and partial soft tissue enthesis attachment to the scaffold (Fig. 7). The average thickness of the soft tissue attachment was significantly less compared with that of the sheep who only had a soft tissue connection (i.e., 0.3–0.5 mm, average 0.4 mm, and 0.5–0.9 mm, average 0.7 mm, respectively) (Table 4). In one of these three sheep, the type of tissue that was preserved on the LPM stump during per-operative fixation was unclear; the bony enthesis was preserved in the other two sheep.

In two sheep, there was uniquely bony ingrowth of the enthesis into the scaffold (Fig. 8). In one of these ewes, per-operative reconstruction of the enthesis was performed using fibrocartilaginous tissue. In the other ewe, it was unclear whether a bony or fibrocartilaginous reconstruction had been achieved.

No significant difference could be found between the sheep that had a bony part of the enthesis attached to the scaffold and the sheep in which an approximation of fibrocartilaginous tissue was achieved, with concern to the formation of either a new bony or soft tissue connection ($p>0.05$).

In 10 of 13 sheep, an additional bony connection between the mandible and the reattached LPM was found below the ostectomy line (Fig. 9). In one of the remaining three sheep, this connection could not be found due to post-mortem dissection too close to the implant that resulted in loss of tissue medial to the implant.

In four sheep, an aseptic loosening and subsequent displacement of the fossa was found (Table 5). In three out of four sheep, a latero-inferior displacement occurred, while in one ewe, an infero-dorsal displacement was seen. All four sheep developed heterotopic ossification surrounding the displaced fossa component, reaching towards the mandibular component. Nevertheless, the bearing surface as well as function of the TMJ remained intact in these sheep.

4. Discussion

Food particles need to be broken down to pieces smaller than 1 mm, in order to be swallowed. The first breakdown of these food particles occurs during initial chewing, followed by chewing during rumination (Domingue et al., 1991). Sheep spend about 4 h per day eating and about 8 h ruminating (Domingue et al., 1991). This masticatory movement is heavily dependent on laterotrusive movement, which is generated through what Allouch calls “the unilateral group” (Parker, 1983; Allouch, 2018). This group of masticatory muscles includes the medial and lateral pterygoid muscle. These structures are also referred to as the internal and external pterygoid muscle, respectively. The latter inserts onto the medial surface of the mandible (above the mandibular foramen) and onto the condyle and disc (Parker, 1983). While the internal/medial pterygoid muscle brings the mandible into a medial and upward position, the external/LPM creates a protrusive movement, as in humans. This muscle and its insertion were dissected intra-operatively and reattached onto the prosthesis.

When placing a TMJR with loss of the LPM, a test subject could lose a significant amount of weight due to reduced laterotrusive function that results in a loss of masticatory efficiency. This outcome did not occur in this group of sheep.

In humans, the lateral pterygoid muscle consists of a superior and inferior belly. It is the only masticatory muscle with horizontally oriented fibers (Stöckle et al., 2019). Murray et al. suggested that the inferior part can be further divided into four zones. They used fine-wire electrodes to measure LPM activity and found a total of 374 single motor units (Murray et al., 2007). The superomedial part initiates protrusive and contralateral movements, and the superolateral and inferomedial parts follow through with these movements. The specific function of the inferolateral part has not been determined. The generally accepted hypothesis is that the superior belly has a role in retrusive movements and closing of the jaw, but Murray et al. (2007) found this hypothesis to be false. They

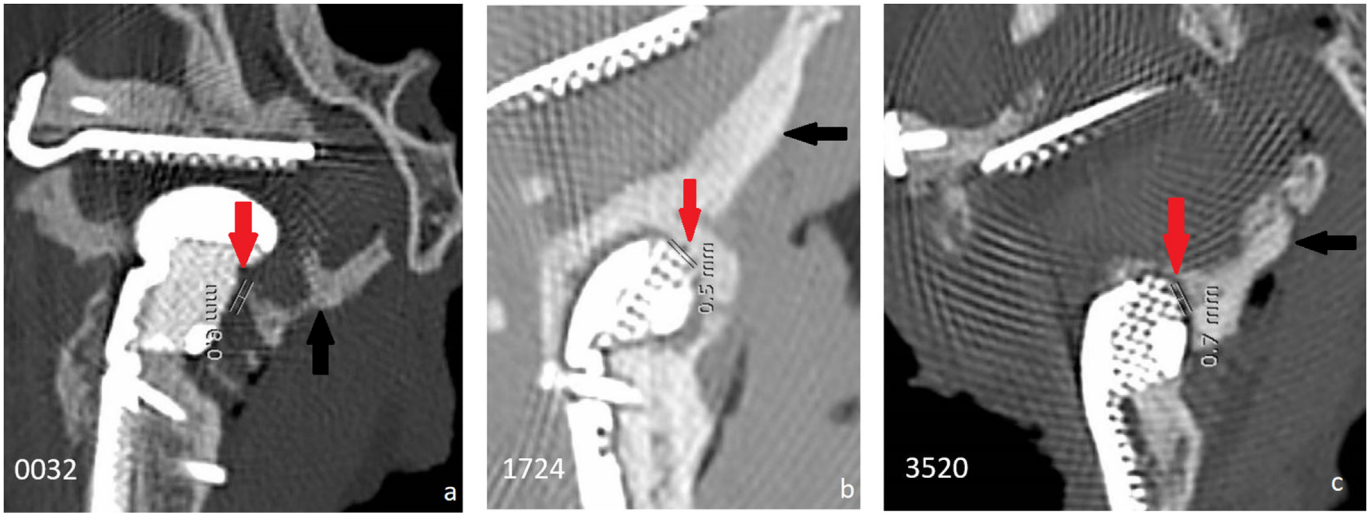

Fig. 6. Soft tissue connection between lateral pterygoid muscle (LPM) and the implant scaffold with measurement. (a) Sheep no. 0032; (b) Sheep no. 1724; (c) sheep no. 3520. Red arrow: soft tissue connection between the LPM enthesis and scaffold. (a) 0.9 mm; (b) 0.5 mm; (c) 0.7 mm. Black arrow: partial calcification of the LMP.

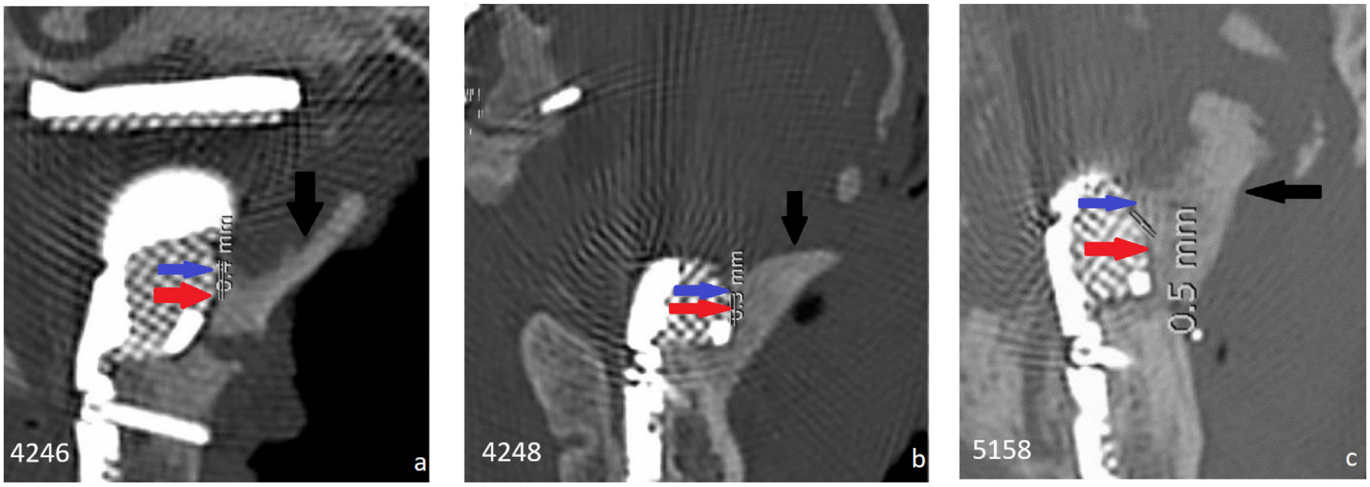

Fig. 7. Partially soft tissue connection between lateral pterygoid muscle (LPM) and the implant scaffold with measurement. (a) Sheep no. 4246; (b) sheep no. 4248; (c) sheep no. 5158. Red arrow: partial soft tissue connection between the LPM enthesis and scaffold. (a) 0.4 mm; (b) 0.3 mm; (c) 0.5 mm. Blue arrow: bony connection between the LPM and the implant scaffold. Black arrow: partial calcification of the LPM.

Table 4
Radiological distance between implant scaffold and bony attachment of the lateral pterygoid muscle (LPM).

Sheep no.	Distance implant – bony insertion
3520	0.7 mm
0032	0.9 mm
1724	0.5 mm
5158	0.5 mm
4246	0.4 mm
4248	0.3 mm

found that the superior belly also participates in contralateral and protrusive movements. The medial part does not display any additional activity, but the lateral part also activates during retrusion and closure of the mouth. Using EMG-based research, Huang et al. (2005) also found that the inferior belly is the principal muscle for laterotrusive movement when the teeth are in contact; the other masticatory muscles have at most a facilitatory role.

To our knowledge, there are only two articles that discuss the reinsertion of the lateral pterygoid muscle when placing a TMJR. Collins et al. (2003) attempted to reattach the lateral pterygoid muscle below the point of the condylectomy in 20 joints. They then compared functionality to four joints in which no reconstruction was performed. They performed a condylectomy and dissected the LPM from the anterior aspect of the condyle, then fixed the muscle to the anterior aspect of the condylar neck in the sigmoid notch region using 2 No 0 polyglactine 910 (Vicryl Ethicon, Sommverville, NJ, USA) sutures. They found significant differences in both laterotrusive and protrusive movements between the two patient groups; the patients who had a reconstruction had a better outcome. Despite these positive results, this research group did not publish more studies on this topic (Collins et al., 2003). When Mommaerts (2019) examined the reconstruction of the LPM enthesis, on which this experiment was based, he found that a reinsertion of the LPM was possible, given the use of a titanium lattice structure in the condylar neck to allow for bony ingrowth.

When attempting to create bony ingrowth into a scaffold, specific conditions must be met to achieve a good outcome. The implant and scaffold surfaces need to be sufficiently osteoconductive to stimulate bone cell growth. The environment also needs to be osteoinductive to promote differentiation of mesenchymal stem cells (MSCs) into (pre)osteoblasts. Good osteogenesis also must also be achieved (i.e., sufficient MSCs, osteoblasts, and osteocytes need to be present). In a natural situation, the mandible is covered by periosteum; however, when performing a resection and placing an implant, the periosteum can be lost. This difference is important, because the inner layer of the periosteum (i.e., the cambium) includes differentiated osteogenic progenitor cells, fibroblasts, and osteoblasts (Dwek, 2010; Lin et al., 2014). The cambium has significant osteoblastic potential, which has a role during fracture healing. However, not all bones are covered by periosteum. Sesamoid bones (e.g., the patella) are not covered by periosteum, but are capable of osseous healing after a fracture (Andersen, 1961). As described by both Shapiro (2008) and Colnot (2009), several types of bone repair can occur after a fracture. The first and primary type is endochondral; a hematoma forms around the fracture, which is stabilized by the periosteum and the surrounding soft tissues. Cells from the cambium start proliferating and differentiating, and membranous ossification starts at the periphery of the fracture. Meanwhile, a central mass of cartilage is also formed. This mass ossifies via endochondral ossification. A clear periosteal reaction can be observed on radiographs. This type of repair can still occur during conditions of macro- or micromotion.

In the case of absence of periosteum and absence of motion, osteoprogenitor cells are derived directly from the Haversian canals when there is direct contact between the two bony pieces. This type of healing is “contact repair.” If there is a gap between the two pieces, lamellar bone is formed directly or woven bone is formed first and then transformed into lamellar bone if the gap is larger. This type of bone repair is also known as (direct) transformational bone repair (Shapiro, 2008).

Periosteum was not preserved in our sheep surgeries, and there were no Haversian canals on the prosthetic side. Therefore, only transformational bone repair can occur as a possible form of repair with associated osseointegration of the LPM tendon. This means that the material to which the LPM attaches must be osteoinductive and osteoconductive. Compared with cobalt-chromium-molybdenum alloy, the elasticity of titanium alloy Gr 23 is closer to that of bone. Its roughened surface has good biocompatibility and is osteoconductive (Polo-Corrales et al., 2014). Titanium is considered a bio-inert material that does not possess any osteoinductive properties. However, Tamaddon et al. (2017) performed in vitro and in vivo experiments and found that even untreated porous titanium scaffolds can be osteoinductive. Many studies have

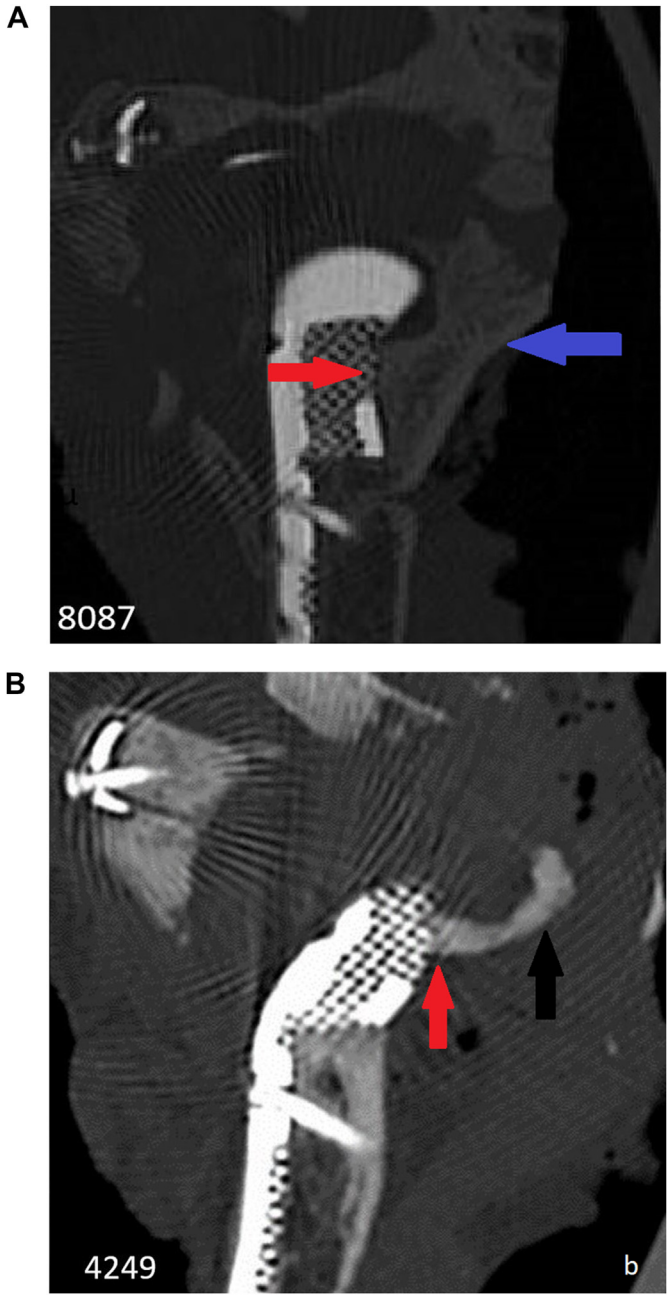

Fig. 8. Bony connection between lateral pterygoid muscle (LPM) and the implant scaffold. (a) Sheep no. 8087; (b) sheep no. 4249. Red arrow: bony connection between the LPM and the implant scaffold; black arrow: partial calcification of the LPM; Blue arrow: significant calcification of the LPM.

found that as surface roughness increases, the connection between the implant and the adjacent bone becomes stronger. Yeniyol et al. (2013) found that oxalic acid etching improves surface roughness by creating micro-pitting. It also improves cell adhesion, which allows for better osteogenesis. The use of ELI-23 titanium allowed for both an osteoinductive and osteoconductive environment, which also allows cementless fixation of titanium implants in orthopedic surgery (Cross et al., 2014; Konttinen et al., 2014).

Sufficient numbers of MSCs, osteoblasts, and osteocytes needed to be present after the periosteum was stripped during the resection. Therefore, part of the resected bone was ground, mixed with a fibrin sealant and applied to the scaffold to provide high concentrations of osteoinductive cells. Spalthoff et al. (2015) found that bone marrow aspirate (BMA) provides an abundant and reliable source of growth factors and osteogenic cells. They examined the use of β-tricalcium phosphate (β-TCP) as a matrix material for seeding and which specific osteogenic cells can improve osteoinductivity. They found that in the group where the β-TCP cylinders were mixed with BMA mixed with crushed bone, the β-TCP is largely replaced with osseous tissue and the cylinder becomes hard and inflexible. The use of venous blood or solely BMA results in significantly less or even no bone formation. They concluded that the combined use of cancellous bone and BMA provides the best results for in vivo heterotopic bone regeneration (Spalthoff et al., 2018). Mommaerts (2019) applied this technique in humans but one of the downsides to BMA usage is that it is an expensive procedure. One of our goals was to exclude the use of MSCs and bone marrow aspirate (BMA) at the scaffold site, to evaluate if it has any merit over only using autologous grounded bone, to establish a reconnection of the enthesis.

While all three factors for bone regeneration and integration were mostly provided, only two of the sheep had radiological bone formation that was up against the scaffold. There was no formation of soft tissue in between the scaffold and the enthesis. Three sheep had a connection that was both soft tissue and bony.

A first remark that has to be made concerning these findings, is the spherical hindrance by the UHMWPE part of the fossa during surgery. While the height was reduced, there was still some difficulty as to achieve proper positioning of the LPM enthesis. Due to the height and width, other than in its human counterpart, it was not always possible to evaluate if the fixation of the enthesis was directly against the scaffold, forming a potential cause for non-integration.

Furthermore, in addition to creating an optimal environment for osteogenesis, implant stability is also important. Pilliar et al. (1986) and Burke et al. (1991) found that movement between the bone and the implant should be less than 28 mμ for bone ingrowth to occur. Fibrous tissue can form if movement is more than 150 mμ, especially when repetitive micromotion occurs. During orthopedic surgery, large compressive forces are applied to achieve good fixation to prevent the forces to which the implant is exposed to during post-operative loading from exceeding the forces necessary to dislodge the implant. The amount of stability can be increased by increasing surface roughness and the total contact surface between the implant and the bony surface (limited in our experiment). In the absence of good initial stability, successful osseointegration between the implant and its bony contact surface will be severely limited (Karrholm et al., 1997).

This was a significant limitation of our experiment, because it was impossible to prevent the sheep from performing laterotrusive movements using their LPMs. Activation of this muscle can create micromovements between the enthesis attachment and the implant scaffold and result in insufficient stability. This relationship seems relevant to three out of five of the sheep. Interconnecting heterotopic ossification (HO) was found around the lateral sides of both the fossa and mandible, which possibly resulted in additional stabilization between the LPM and implant. However, this finding was not present for the other two sheep that had (partial) bony reattachment of the LPM enthesis, no displacement of the fossa, nor any heterotopic bone formation (Table 5). Unlike sheep, humans can be asked to consume a liquid to soft diet and only perform depression and elevation of the mandible during the first 6 weeks after surgery. This restriction can prevent LPM micromovements and maximize the chances of good ingrowth. However, restoration of the maximal “range of motion” during the post-operative recovery period could be delayed (De Meurechy et al., 2019). While a limitation in movement might lead to concerns with regard to HO

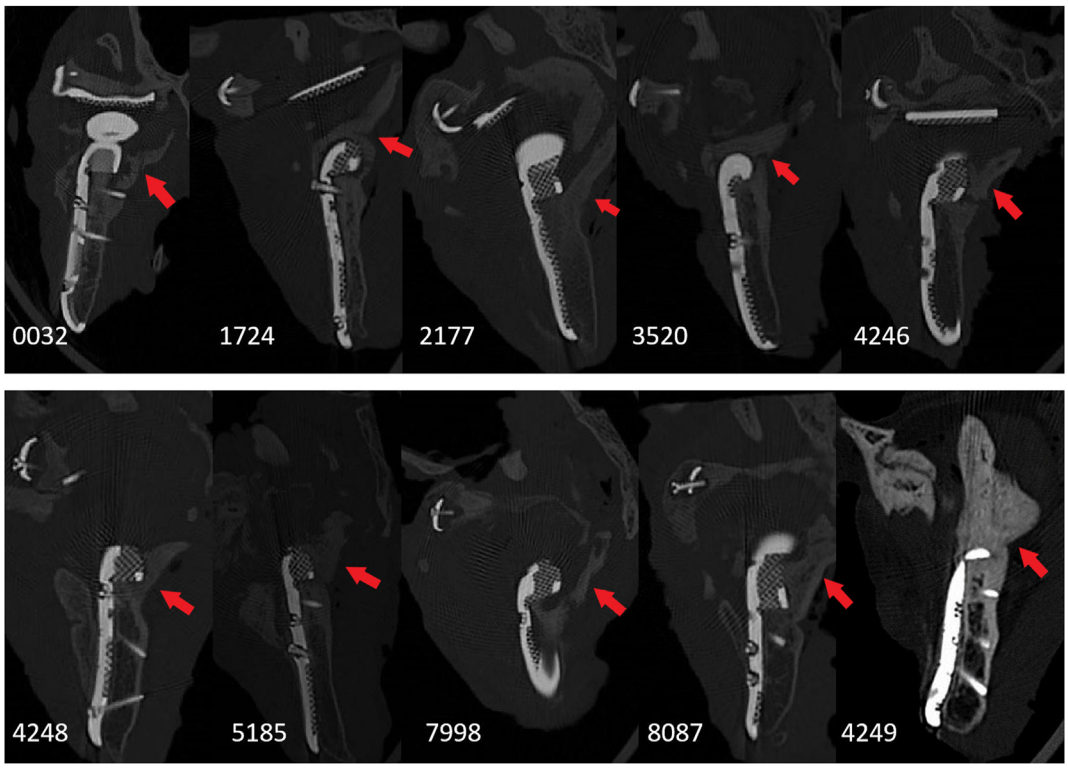

Fig. 9. Bony connection between the enthesis and mandible. Red arrow: bony connection between the lateral pterygoid muscle (LPM) and the mandible.

Table 5
Fossa and ramal component positioning.

Sheep no.	Ramal component	Fossa component
3520	Normal	Normal
8087	Normal with lateral incapsulation	Normal with heterotopic bone formation
2177	Normal	Latero-inferior displacement with heterotopic bone incapsulation
5158	Normal with lateral incapsulation	Infero-dorsal displacement with heterotopic bone incapsulation
2549	Normal	Normal
4249	Normal	Normal
0032	Normal	Normal
7998	Normal	Latero-inferior displacement with heterotopic bone incapsulation
4246	Normal	Normal
1724	Normal	Normal
4248	Normal with lateral incapsulation	Latero-inferior displacement with heterotopic bone incapsulation
8787	Normal	Normal
4473	Normal	Normal
0075	Sham	Sham

and possible ankylosis, several remarks have to be made. First, none of the patients that were included in the study by Mommaerts (2019) that were treated with LPM reinsertion, showed heterotopic bone formation. Second, with consideration of the peroperative difficulties that were experienced as to evaluate if the enthesis came in direct contact with the subcondylar lattice structure, sometimes residual bone chips were added to the assumed gap. This in turn might have led to a hyperostotic reaction in some sheep.

Third, evidence seems to indicate that by filling out the negative space around the joint, by means of an autologous fat graft for instance, the risk of heterotopic ossification can be reduced as well (Van Bogaert et al., 2018). Finally, while five ewes developed heterotopic bone formation, four of these sheep presented themselves with an aseptic loosening and subsequent displacement of the fossa (Table 5). Despite the fossa being designed to achieve a perfect anatomical fit, the aseptic loosening most likely occurred due to micromovements between the fossa and the underlying bone. This resulted in bone resorption underneath the titanium surface of the fossa (Shen et al., 2014). A possible cause was the use of 2 mm diameter screws for fixation of the zygomatic component. Considering the higher mastication rate and mainly laterotrusive movement, the fossa is subjected to higher forces compared to its human counterpart. While a higher screw diameter increases the fatigue resistance and lessens the risk of failure as excessive stress in the bone surrounding the screw, the opposite is true for screws with a smaller diameter (Skinner et al., 1990; Chaudhary et al., 2008). This excessive stress can lead to bone resorption and implant failure (Tada et al., 2003; Shen et al., 2014). As a result, using 2-mm-diameter screws under this higher load compared to its human counterpart, can very well have resulted in insufficient fixation of the fossa in four out of 13 ewes. Furthermore, in humans

a soft diet can be maintained during the period of osseointegration, limiting the amount of force the TMJ is subjected to. While no loosening or displacement of the fossa component was seen in humans (Mommaerts, 2019), further trials in humans are needed to support this statement.

Although no evidence is available concerning HO following TMJ implant displacement, a significant effect was found between the occurrence of HO and the displacement of the fossa component ($p < 0.01$). As trauma and fractures have been validated as causes for HO in orthopedic literature (Nauth et al., 2012), as well as TMJ ankylosis (Yan et al., 2014), we would advise not to apply this technique of enthesis reconstruction in young patients, nor in patients with an ankylotic joint. This to avoid any risk of (re-)ankylosis, until further trials in humans are done.

The effects of imaging artifacts should also be considered. Because the TMJR was completely made of titanium, artifacts that caused decreases in image quality might have affected the results. Titanium has a high density, so low-energy photons are more absorbed than high-energy photons, leading to beam hardening (Wellenberg et al., 2018). This effect is even more apparent between an implant and other high density materials or tissue such as bone (Zhao et al., 2000). When photons change direction they can end up in the wrong detector, which results in dark streaks in the areas of photon loss (Wellenberg et al., 2018). These artifacts can lead to blurred inaccurate images (Zhang et al., 2011; Wellenberg et al., 2018). Limiting these artifacts was attempted by decreasing the reconstruction thickness, as proposed by Moon et al. (2008). However, the kilovoltage was 120 kV, and an increase to 140 kV might have resulted in further reduction of metal artifacts (Moon et al., 2008). A metal artifact-reducing sequence (MARS algorithm) was used as to improve the image during processing. Nevertheless, due to the high density and possibly due to the irregular shape of the scaffold, current artifact removal software is unable to completely remove artifacts (Wellenberg et al., 2018). The darkened areas can reduce the accuracy of the evaluation between the reconstructed enthesis and the implant, and increase the need for histological analysis of the scaffold and enthesis insertion.

Despite only five sheep showing ingrowth of the bone into the scaffold, the LPM remained well-connected in 10 out of 13 sheep, either through the formation of an attachment to the scaffold, and/or due to the lateral pterygoid muscle reinserting on the mandibular bone below the osteotomy.

These sheep had good laterotrusive movement and clinical function. The typology of the enthesis provides one explanation for these findings. According to Benjamin et al. (2002) there are two types of enthesis (i.e., fibrous and fibrocartilaginous). Fibrous entheses are present in several large muscles (e.g., the deltoid muscle) and are less prone to overuse compared to fibrocartilaginous entheses. This group is then further divided into the periosteal and the bony types, which attach to the periosteum or directly into the bone. Based on the cinematic imaging results, weights, and radiological findings, the findings for our sheep might have been affected by this type of enthesis. Further histological analysis of enthesis reconstruction is needed.

In sheep, the masseteric muscle can be dissected into three distinct layers. The most extensive layer also exerts a protrusive force (Parker, 1983). This characteristic suggests that the laterotrusive movements seen during the clinical analysis were due to these fibers rather than the LPM. However, the previously discussed evidence negates this argument.

When using larger and more complex scaffolds, sufficient blood supply is needed to provide adequate nutrition to the osteogenic cells (Laschke et al., 2008; Kokemueller et al., 2010). The outer layer of the periosteum mainly consists of collagen and fibroblasts, but it also contains the highest density of blood vessels and provides vascularization to adjacent bone and muscle (Allen et al., 2004). The use of periosteal flaps and free periosteal grafts to provide vascularization and an osteoinductive and conductive environment to bone grafts is not new (Lin et al., 2014; Hernigou, 2015). In 10 out of 13 sheep, a bony connection was formed between the osseous mandible and the enthesis. Important to notice is that the distance from the insertion of the muscle to the bony mandibular margin was much smaller in the TMJR that were placed, compared to the design for human use. This was due to a reduced height of the condylar neck in the implants that were placed. As such it is possible that ~~that~~ this bony connection was formed due to the periosteal sleeve still being intact, providing not only the necessary environment for bone formation to occur, but also the necessary vascularity, which might have been absent near the scaffold. Gallardo-Calero et al. (2019) found that intramembranous ossification occurs in areas where a bony defect is covered with a vascularized periosteal flap. However, Leucht et al. (2008) found that intramembranous ossification occurs when mandibular periosteum is transplanted onto a tibial bony defect. Endochondral ossification occurs when tibial periosteum is transplanted onto a mandibular defect. These findings indicate that the origin of the periosteum affects the repair. Leucht et al. (2008) concluded that in craniomaxillofacial and orthopedic surgeries, regardless of the origin of the periosteum, it allows for bone regeneration independent of the type of repair that occurs. Therefore, the preservation of periosteal tissue could be considered to maximize the possibility of bony integration of the enthesis into the scaffold. However, because a soft diet and restriction in movement can be applied in humans, inclusion of a surgically-difficult vascularized periosteal flap might not be necessary, urging the need for trial in humans with strict limitations on laterotrusion during the first 6 post-operative weeks.

A first limitation we encountered in this study were the difficulties with concern to the reattachment of the LPM. While these were mainly due to the anatomical differences of the sheep's TMJ compared to its human counterpart, these could be facilitated by providing muscle relaxant medication during surgery, when performing the condylectomy. A second solution could be to alter the design of the condylar component, by adding an extension at the level of the neck with a lattice structure. This can help reduce the distance between the scaffold and the tendon, allowing for an easier fixation.

A second significant limitation we encountered during our research, was the impossibility to limit immediate post-operative laterotrusive movement, as previously discussed. In human patients, besides prohibiting laterotrusive movements for purpose of rehabilitation, a liquid to soft diet is indicated for at least 3 weeks in the post-operative phase. In the present study a similar dietary program could not be implemented considering the particular ruminant digestive anatomy and physiology that cannot sustain longer periods of lack of roughage due to risk of dysbacteriosis (Hoover and Miller (1991)). This limited the duration of dietary restrictions to only 1 week after implantation.

Finally, the exact typology of the enthesis reconstruction (i.e., fibrous and fibrocartilaginous) could not be determined by means of radiological imaging. In order to gain a more complete insight into this matter, further histological analysis will be conducted.

5. Conclusion

The study shows great promise for improvements upon the current approach to TMJR in terms of replacing the joint itself and reconstruction of the lateral pterygoid muscle's insertion and function. However, enthesis reconstruction is most likely not warranted in young children, nor in cases of TMJ ankylosis, because of risk of (re)ankylosis. Further optimization of the reattachment

technique and scaffold position and surface area should be done, as well as trials in humans as to evaluate the effect of proper revalidation.

Funding

This work was supported by VLAIO (Grant number HBC.2018.0093). They had no involvement in the collection, analysis nor interpretation of the data, nor in the writing of the report or decision to submit the article for publication.

Declaration of competing interest

Mommaerts, MY is co-owner and innovation manager at CAD-Skills BV. All the other.

References

Allen, M.R., Hock, J.M., Burr, D.B., 2004. Periosteum: biology, regulation, and response to osteoporosis therapies. Bone 35, 1003–1012.
Allouch, M.G., 2018. Functional anatomy of the masticatory mechanism: a comparative study of physical characteristics of jaw-unilateral muscles in sheep. Int J Vet Sci 7, 134–139.
Andersen, H., 1961. Histochemical studies on the histogenesis of the knee joint and superior tibio-fibular joint in human foetuses. Acta Anat (Basel) 46, 279–303.
Ângelo, D.F., Gil, F.M., González-García, R., Mónico, L., Sousa, R., Neto, L., et al., 2018. Effects of bilateral discectomy and bilateral discopexy on black Merino sheep rumination kinematics: TEMPOJIMS – phase 1 – pilot blinded, randomized preclinical study. J Craniomaxillofac Surg 46, 346–355.
Ângelo, D.F., Morouço, P., Alves, N., Viana, T., Santos, F., González, R., et al., 2016. Choosing sheep (Ovis aries) as animal model for temporomandibular joint research: morphological, histological and biomechanical characterization of the joint disc. Morphologie 100, 223–233.
Bates, J.F., Stafford, G.D., Harisson, A., 1976. Masticatory function—a review of the literature. J Oral Rehabil 3 (57–67).
Benjamin, M., Kumai, T., Milz, S., Boszczyk, B.M., Boszczyk, A.A., Ralphs, J.R., 2002. The skeletal attachment of tendons—tendon "entheses.". Comp Biochem Physiol - A Mol Integr Physiol 133, 931–945.
Burke, D.W., Bragdon, C.R., Jasty, M., Haire, T., Harris, W.H., 1991. Dynamic measurement of interface mechanics in vivo and the effect of micromotion on bone ingrowth into a porous surface device under controlled loads in vivo. In: 37th annual meeting of orthopaedic research society, anaheim, CA, p. 103.
Chaudhary, N., Lovald, S.T., Wagner, J., Khraishi, T., Baack, B., 2008. Experimental and numerical modeling of screws used for rigid internal fixation of mandibular fractures. Model Simulat Eng 3, 1–11.
Collins, C.P., Wilson, K.J., Collins, P.C., 2003. Lateral pterygoid myotomy with reattachment to the condylar neck: an adjunct to restore function after total joint reconstruction. Oral Surg Oral Med Oral Pathol Oral Radiol Endod 95, 672–673.
Colnot, C., 2009. Skeletal cell fate decisions within periosteum and bone marrow during bone regeneration. J Bone Miner Res 24, 274–282.
Cross, M.J., Roger, G.J., Spycher, J., 2014. Cementless fixation techniques and challenges in joint replacement. In: Revell, P.A. (Ed.), Joint replacement technology, 2nd ed. Woodhead Publishing, pp. 186–211.
De Meurechy, N., Mommaerts, M.Y., 2018. Alloplastic temporomandibular joint replacement systems: a systematic review of their history. Int J Oral Maxillofac Surg 47, 743–754.
De Meurechy, N., Loos, P.-J., Mommaerts, M.Y., 2019. Postoperative physiotherapy after open temporomandibular joint surgery: a 3-step program. J Oral Maxillofac Surg 77, 932–950.
Dimitroulis, G., 2014. Comparison of the outcomes of three surgical treatments for end-stage temporomandibular joint disease. Int J Oral Maxillofac Surg 43, 980–989.
Domingue, B.M., Dellow, D.W., Barry, T.N., 1991. The efficiency of chewing during eating and ruminating in goats and sheep. Br J Nutr 65, 355–363.
Dwek, J.R., 2010. The periosteum: what is it, where is it, and what mimics it in its absence? Skeletal Radiol 39, 319–323.
Elledge, R., Mercuri, L.G., Attard, A., Green, J., Speculand, B., 2019. Review of emerging temporomandibular joint total joint. Br J Oral Maxillofac Surg 57, 722–728.
Gallardo-Calero, I., Barrera-Ochoa, S., Manzanares, M.C., Sallent, A., Vicente, M., López-Fernández, A., et al., 2019. Vascularized periosteal flaps accelerate osteointegration and revascularization of allografts in rats. Clin Orthop Relat Res 477, 741–755.
Hernigou, P., 2015. Bone transplantation and tissue engineering. Part II: bone graft and osteogenesis in the seventeenth, eighteenth and nineteenth centuries (Duhamel, Haller, Ollier and MacEwen). Int Orthop 39, 193–204.
Hoover, W.H., Miller, T.K., 1991. Rumen digestive physiology and microbial ecology. Vet Clin North Am Food Anim Pract 7, 311–325.
Huang, B.Y., Whittle, T., Murray, G.M., 2005. Activity of inferior head of human lateral pterygoid muscle during standardized lateral jaw movements. Arch Oral Biol 50, 49–64.
Karrholm, J., Herberts, P., Hultmark, P., Malchau, H., Nivbrant, B., Thanner, J., 1997. Radiostereometry of hip prostheses. Review of methodology and clinical results. Clin Orthop Relat Res 94–110.
Kijak, E., Margielewicz, J., Lietz-Kijak, D., Wilemska-Kucharzewska, K., Kucharzewski, M., Śliwiński, Z., 2017. Model identification of stomatognathic muscle system activity during mastication. Exp Ther Med 13, 136–145.
Kokemueller, H., Spalthoff, S., Nolff, M., Tavassol, F., Essig, H., Stuehmer, C., et al., 2010. Prefabrication of vascularized bioartificial bone grafts in vivo for segmental mandibular reconstruction: experimental pilot study in sheep and first clinical application. Int J Oral Maxillofac Surg 39, 379–387.
Konttinen, Y.T., Milošev, I., Trebše, R., van der Linden, R., Pieper, J., Sillat, T., 2014. Metals for joint replacement. In: Revell, P.A. (Ed.), Joint replacement technology, 2nd ed. Woodhead Publishing, pp. 81–151.
Laschke, M.W., Rucker, M., Jensen, G., Carvalho, C., Mulhaupt, R., Gellrich, N.-C., et al., 2008. Improvement of vascularization of PLGA scaffolds by inosculation of in situ-preformed functional blood vessels with the host microvasculature. Ann Surg 248, 939–948.
Leucht, P., Kim, J.-B., Amasha, R., James, A.W., Girod, S., Helms, J.A., 2008. Embryonic origin and Hox status determine progenitor cell fate during adult bone regeneration. Development 135, 2845–2854.
Lin, Z., Fateh, A., Salem, D.M., Intini, G., 2014. Periosteum: biology and applications in craniofacial bone regeneration. J Dent Res 93, 109–116.
Mercuri, L.G., Wolford, L.M., Sanders, B., Dean White, R., Giobbie-Hurder, A., 2002. Long-term follow-up of the CAD/CAM patient fitted total temporomandibular joint reconstruction system. J Oral Maxillofac Surg 60, 1440–1448.
Mommaerts, M.Y., 2019. On the reinsertion of the lateral pterygoid tendon in total temporomandibular joint replacement surgery. J Craniomaxillofac Surg 47, 1913–1917.
Moon, S.G., Hong, S.H., Choi, J.-Y., Jun, W.S., Kang, H.-G., Kim, H.-S., et al., 2008. Metal artifact reduction by the alteration of technical factors in multidetector computed tomography: a 3-dimensional quantitative assessment. J Comput Assist Tomogr 32, 630–633.
Murray, G.M., Bhutada, M., Peck, C.C., Phanachet, I., Sae-Lee, D., Whittle, T., 2007. The human lateral pterygoid muscle. Arch Oral Biol 52, 377–380.
Nauth, A., Giles, E., Potter, B.K., Nesti, L.J., O'brien, F.P., Bosse, M.J., et al., 2012. Heterotopic ossification in orthopaedic trauma. J Orthop Trauma 26, 684–688.
Parker, W.S., 1983. The comparative anatomy of the internal and external pterygoid muscles. Functional variations among species. Angle Orthod 53, 9–18.
Pilliar, R.M., Lee, J.M., Maniatopoulos, C., 1986. Observations on the effect of movement on bone ingrowth into porous-surfaced implants. Clin Orthop Relat Res 108–113.
Polo-Corrales, L., Latorre-Esteves, M., Ramirez-Vick, J.E., 2014. Scaffold design for bone regeneration. J Nanosci Nanotechnol 14, 15–56.
Rentsch, C., Schneiders, W., Manthey, S., Rentsch, B., Rammelt, S.S., 2014. Comprehensive histological evaluation of bone implants. Biomatter 4, 1–11.
Shapiro, F., 2008. Bone development and its relation to fracture repair. The role of mesenchymal osteoblasts and surface osteoblasts. Eur Cells Mater 15, 53–76.
Shen, P., Zhang, S., Yang, C., Huang, D., 2014. The mandibular symmetry evaluation of total temporomandibular joint replacement on developing sheep. J Craniomaxillofac Surg 42, 201–205.
Skinner, R., Maybee, J., Transfeldt, E., Venter, R., Chalmers, W., 1990. Experimental pullout testing and comparison of variables in transpedicular screw fixation. A biomechanical study. Spine 15, 195–201.
Spalthoff, S., Jehn, P., Zimmerer, R., Mollmann, U., Gellrich, N.-C., Kokemueller, H., 2015. Heterotopic bone formation in the musculus latissimus dorsi of sheep using beta-tricalcium phosphate scaffolds: evaluation of an extended prefabrication time on bone formation and matrix degeneration. Int J Oral Maxillofac Surg 44, 791–797.
Spalthoff, S., Zimmerer, R., Dittmann, J., Kokemüller, H., Tiede, M., Flohr, L., 2018. Heterotopic bone formation in the musculus latissimus dorsi of sheep using β-tricalcium phosphate scaffolds: evaluation of different seeding techniques. Regen Biomater 5, 77–84.
Stöckle, M., Fanghänel, J., Knüttel, H., Alamanos, C., Behr, M., 2019. The morphological variations of the lateral pterygoid muscle: a systematic review. Ann Anat 222, 79–87.
Tada, S., Stegaroiu, R., Kitamura, E., Miyakawa, O., Kusakari, H., 2003. Influence of implant design and bone quality on stress/strain distribution in bone around implants: a 3-dimensional finite element analysis. Int J Oral Maxillofac Implant. 18, 357–368.
Tamaddon, M., Samizadeh, S., Wang, L., Blunn, G., Liu, C., 2017. Intrinsic osteoinductivity of porous titanium scaffold for bone tissue engineering. Int J Biomater 1–11.
Van Bogaert, W., De Meurechy, N., Mommaerts, M.Y., 2018. Autologous fat grafting in total temporomandibular joint replacement surgery. Ann Maxillofac Surg 8, 299–302.
Verplancke, K., De Waele, W., De Bruyn, H., 2011. Dental implants, what should be known before starting an in vitro study. Conf Sustain Constr Des 2, 360–369.
Wellenberg, R.H.H., Hakvoort, E.T., Slump, C.H., Boomsma, M.F., Maas, M., Streekstra, G.J., 2018. Metal artifact reduction techniques in musculoskeletal CT-imaging. Eur J Radiol 107, 60–69.

Yan, Y.B., Liang, S.X., Shen, J., Zhang, J.-C., Zhang, Y., 2014. Current concepts in the pathogenesis of traumatic temporomandibular joint ankylosis. Head Face Med 10, 35.

Yeniyol, S., Bölükbaşi, N., Çakir, A.F., Bilir, A., Ozdemir, T., 2013. Effects of surface modifications with oxalic acid etching and sandblasting on surface topography and biocompatibility of cpTi surfaces. Biotechnol Biotechnol Equip 27, 3995–4001.

Zhang, X., Wang, J., Xing, L., 2011. Metal artifact reduction in x-ray computed tomography (CT) by constrained optimization. Med Phys 38, 701–711.

Zhao, S., Robertson, D.D., Wang, G., Whiting, B., Bae, K.T., 2000. X-ray CT metal artifact reduction using wavelets: an application for imaging total hip prostheses. IEEE Trans Med Imaging 19, 1238–1247.